Precision Rosenbluth Measurement of the Proton Elastic Form Factors

I. A. Qattan,[1,2] J. Arrington,[2] R. E. Segel,[1] X. Zheng,[2] K. Aniol,[3] O. K. Baker,[4] R. Beams,[2] E. J. Brash,[5] J. Calarco,[6] A. Camsonne,[7] J.-P. Chen,[8] M. E. Christy,[4] D. Dutta,[9] R. Ent,[8] S. Frullani,[10] D. Gaskell,[11] O. Gayou,[12] R. Gilman,[13,8] C. Glashausser,[13] K. Hafidi,[2] J.-O. Hansen,[8] D. W. Higinbotham,[8] W. Hinton,[14] R. J. Holt,[2] G. M. Huber,[5] H. Ibrahim,[14] L. Jisonna,[1] M. K. Jones,[8] C. E. Keppel,[4] E. Kinney,[11] G. J. Kumbartzki,[13] A. Lung,[8] D. J. Margaziotis,[3] K. McCormick,[13] D. Meekins,[8] R. Michaels,[8] P. Monaghan,[9] P. Moussiegt,[15] L. Pentchev,[12] C. Perdrisat,[12] V. Punjabi,[16] R. Ransome,[13] J. Reinhold,[17] B. Reitz,[8] A. Saha,[8] A. Sarty,[18] E. C. Schulte,[2] K. Slifer,[19] P. Solvignon,[19] V. Sulkosky,[12] K. Wijesooriya,[2] and B. Zeidman[2]

[1]*Northwestern University, Evanston, Illinois 60208, USA*
[2]*Argonne National Laboratory, Argonne, Illinois 60439, USA*
[3]*California State University at Los Angeles, Los Angeles, California 90032, USA*
[4]*Hampton University, Hampton, Virginia 23668, USA*
[5]*University of Regina, Regina, Saskatchewan, Canada, S4S 0A2*
[6]*University of New Hampshire, Durham, New Hampshire 03824, USA*
[7]*Université Blaise Pascal Clermont-Ferrand et CNRS/IN2P3 LPC 63, 177 Aubière Cedex, France*
[8]*Jefferson Laboratory, Newport News, Virginia 23606, USA*
[9]*Massachusetts Institute of Technology, Cambridge, Massachusetts 02139, USA*
[10]*Istituto Nazionale di Fisica Nucleare, Sezione Sanità, 00161 Roma, Italy*
[11]*University of Colorado, Boulder, Colorado 80309, USA*
[12]*College of William and Mary, Williamsburg, Virginia 23187, USA*
[13]*Rutgers, The State University of New Jersey, Piscataway, New Jersey 08855, USA*
[14]*Old Dominion University, Norfolk, Virginia 23529, USA*
[15]*Laboratorie de Physique Subatomique et de Cosmologie, F-38026 Grenoble, France*
[16]*Norfolk State University, Norfolk, Virginia 23529, USA*
[17]*Florida International University, Miami, Florida 33199, USA*
[18]*Saint Mary's University, Halifax, Nova Scotia, Canada B3H 3C3*
[19]*Temple University, Philadelphia, Pennsylvania 19122, USA*

(Received 7 October 2004; published 15 April 2005)

We report the results of a new Rosenbluth measurement of the proton electromagnetic form factors at Q^2 values of 2.64, 3.20, and 4.10 GeV^2. Cross sections were determined by detecting the recoiling proton, in contrast to previous measurements which detected the scattered electron. Cross sections were determined to 3%, with relative uncertainties below 1%. The ratio $\mu_p G_E/G_M$ was determined to 4%–8% and showed $\mu_p G_E/G_M \approx 1$. These results are consistent with, and much more precise than, previous Rosenbluth extractions. They are inconsistent with recent polarization transfer measurements of similar precision, implying a systematic difference between the techniques.

DOI: 10.1103/PhysRevLett.94.142301 PACS numbers: 25.30.Bf, 13.40.Gp, 14.20.Dh

Reproducing the structure of the proton is one of the defining problems of QCD. The electromagnetic structure can be expressed in terms of the electric and magnetic form factors, G_E and G_M, which depend only on the four-momentum transfer squared, Q^2. They have traditionally been determined utilizing the Rosenbluth formula [1] for elastic e-p scattering:

$$\frac{d\sigma}{d\Omega_e} = \frac{\sigma_{M\text{ott}}}{\varepsilon(1+\tau)}[\tau G_M^2(Q^2) + \varepsilon G_E^2(Q^2)], \qquad (1)$$

where $\tau = Q^2/4M_p^2$, $\varepsilon = 1/[1 + 2(1+\tau)\tan^2(\theta_e/2)]$ is the virtual photon polarization parameter, M_p is the proton mass, and θ_e is the electron scattering angle. The form factors are related to the spatial distributions of the charge and magnetization in the proton, and in the nonrelativistic limit are simply the Fourier transforms of these distributions.

A Rosenbluth separation is performed by varying the incident electron energy and scattering angle to keep Q^2 constant while varying ε. Rosenbluth separations of G_E and G_M have been reported from 1960 to the present day (Refs. [2,3] and references therein). Fits to these data yield $\mu_p G_E/G_M \approx 1$ [2,4], implying similar charge and magnetization distributions. At large Q^2 values, G_M dominates the cross section at all ε values (contributing more than 90% for $Q^2 > 4$ GeV^2) and therefore the uncertainty in G_E increases with increasing Q^2.

The ratio G_E/G_M can be determined in polarization transfer experiments, where longitudinally polarized electrons are scattered from unpolarized protons and both transverse and longitudinal polarization are transferred to the struck proton. Such experiments have been performed

at Jefferson Lab up to $Q^2 = 5.6$ GeV^2 [5,6] and found the ratio decreasing with increasing Q^2, in stark contrast to the approximate scaling observed in Rosenbluth measurements.

At high Q^2, the reported uncertainties on the polarization transfer results are much smaller than those for the Rosenbluth extractions. This fact, combined with the scatter in the results from different Rosenbluth measurements, led to speculation that the Rosenbluth determinations of G_E were unreliable, although the scatter appears to be related to improper treatment of normalization uncertainties when combining multiple data sets [4]. We report here the results of a new experiment that utilizes an improved Rosenbluth technique to determine G_E/G_M with uncertainties comparable to the recent polarization transfer measurements.

Experiment E01-001 was performed in Hall A at Jefferson Laboratory. A 70 μA electron beam with energies from 1.9 to 4.7 GeV impinged on a 4 cm liquid hydrogen (LH2) target. Protons from elastic e-p scattering were detected in the high resolution spectrometer [7]. An aerogel Cerenkov detector was used to eliminate charged pions and data from a "dummy" target were used to measure the contribution from the target walls. Table I lists the kinematics of the experiment.

At large Q^2 values, G_E yields only a small ε-dependent contribution to the cross section, making its extraction sensitive to small ε-dependent corrections. All previous separations involved detection of the electron, where both the cross section and electron momentum vary strongly with ε, meaning that any rate- or momentum-dependent corrections yield significant corrections to the extracted value of G_E. We detected the struck proton, which greatly reduces the effect of such corrections. At fixed Q^2, $d\sigma/d\Omega_p$ changes by less than a factor of 2 over the measured ε range, while $d\sigma/d\Omega_e$ varies by a factor of 100. The proton momentum is constant at fixed Q^2, while the electron momentum varies by a factor of 10. Finally, radiative corrections (mainly electron bremsstrahlung) and the effect of offsets in the beam energy or scattering angle have smaller ε dependence when the proton is detected.

Figure 1 shows two spectra for δp, the difference between the measured proton momentum and the proton momentum expected for elastic scattering at the measured proton angle. The spectrum is dominated by the e-p elastic peak. To allow separation of the elastic peak from other processes, we perform a Monte Carlo simulation of the elastic scattering, taking into account acceptance and resolution of the spectrometer, energy loss, multiple scattering, and radiative corrections [8]. The resolution of the simulation has been modified to reproduce the small non-Gaussian tails observed in the data. These are matched to the coincidence data, taken for two beam energies at $Q^2 = 2.64$ GeV^2, where the backgrounds that dominate the singles spectrum at large $|\delta p|$ are strongly suppressed. While the momentum and angle resolution are constant, the width of the δp spectrum changes because the dependence of the proton momentum on angle grows with ε.

The background extending to high δp (Fig. 1) is due to quasielastic scattering and other reactions in the target walls and contributes $\sim$10% of the events in the region we used to extract the elastic cross section. The remaining background is mainly due to $\gamma p \to \pi^0 p$ events. This background was modeled using a calculated bremsstrahlung spectrum and an s^{-7} cross section dependence, and yields a correction that is always below 2%.

Because the thicknesses are different for the LH2 and dummy targets, the bremsstrahlung yields are also slightly different. We use the dummy data to determine the shape of

TABLE I. Kinematics of the experiment. The beam energy is known to 0.06% and the angle to 0.3 mr.

E_{beam}	$Q^2 = 2.64$ GeV^2		$Q^2 = 3.20$ GeV^2		$Q^2 = 4.10$ GeV^2	
(GeV)	ε	$\theta_p(^\circ)$	ε	$\theta_p(^\circ)$	ε	$\theta_p(^\circ)$
1.912	0.117	12.631	...	...	...	...
2.262	0.356	22.166	0.131	12.525	...	...
2.842	0.597	29.462	0.443	23.395	0.160	12.682
3.772	0.782	35.174	0.696	30.500	0.528	23.666
4.702	0.865	38.261	0.813	34.139	0.709	28.380

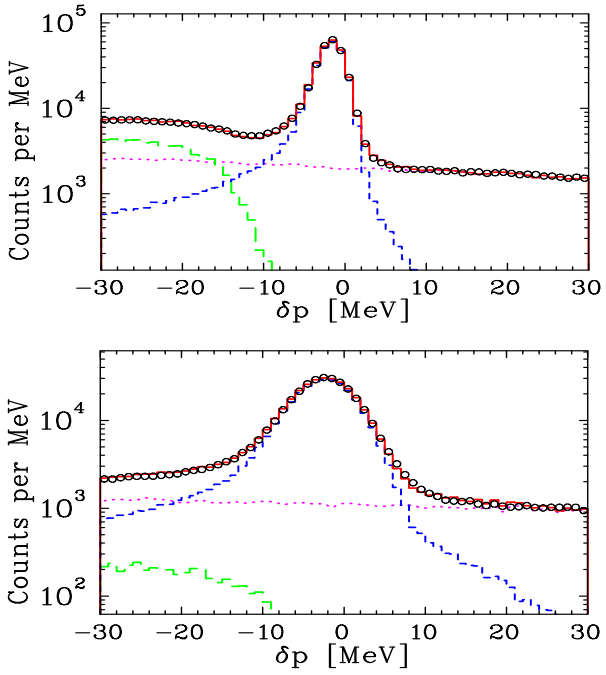

FIG. 1 (color online). The measured δp spectrum for the low (top) and high (bottom) ε points at $Q^2 = 3.2$ GeV^2 (circles). The dotted magenta line is the background from the target walls, the long-dash green line is the simulated background from $\gamma p \to \pi^0 p$ and $\gamma p \to \gamma p$ reactions, the short-dash blue line is the simulated elastic spectrum, and the solid red line (largely obscured by the data points) is the sum of the target wall, elastic, and background contributions.

the end cap contributions, but normalize the contribution to the LH2 spectrum at large δp, where the hydrogen contribution is negligible. While the shape of the bremsstrahlung spectrum differs slightly between the dummy and LH2 targets, the effect is only noticeable near the end point, and a small uncertainty due to this difference is included in the systematic uncertainties.

After removing the end cap background, the simulated spectra from the combination of $\gamma p \to \pi^0 p$ and $\gamma p \to \gamma p$ are normalized to the low-momentum sides of the δp spectra (taking into account the elastic radiative tail). Removing this background yields clean spectra of elastic events. We examine a window in δp around the elastic peak and extract the elastic cross section by taking the value used in the simulation, scaled by the ratio of counts in the data to counts in the simulated spectrum. The upper edge of the window varied from 5 to 15 MeV above the peak, and is scaled with the resolution of the peak. The lower edge goes from 10 to 16 MeV below the peak, and is chosen to minimize the radiative correction while excluding background events. We also varied the δp windows, and the change in the extracted cross sections was consistent with the uncertainties we have assigned to the cut-dependent corrections.

The yield is corrected for dead time in the data acquisition system as well as several small inefficiencies. Corrections for tracking efficiency, trigger efficiency, and particle identification cuts were small ($<2\%$) and independent of ε. About 5% of the protons are absorbed in the target and detector stack, mainly in the hodoscopes and the aerogel detector. We calculate the absorption in the target and detector materials, which is ε independent except for the target absorption which varies by $\ll 0.1\%$. Radiative corrections to the cross section are $\sim 20\%$, with a 5%–10% ε dependence, smaller than in previous Rosenbluth separations where the electron was detected. We also require a single clean cluster of hits in each drift chamber plane to avoid events where the resolution is worsened by noise in the chambers. This reduces the non-Gaussian tails, but leads to an inefficiency of roughly 7%, with a small (0.25%) ε dependence, possibly related to the variation of rate with ε. We correct the yield for the observed inefficiency and apply a 100% uncertainty on the ε dependence of the correction.

The absolute uncertainty on the extracted cross sections is approximately 3%, dominated by corrections for the angular acceptance (2%), radiative processes (1%), proton absorption in the target and detectors (1%), background processes (1%), and the uncertainty in the integrated luminosity (1%). We apply a tight cut on the solid angle, using only the data in the central 1.6 msr of the total ≈ 6 msr acceptance. This cut limits the elastic data to the region of 100% acceptance, but leads to the relatively large uncertainty in the size of the software-defined solid angle. Because the solid angle is identical for all ε values at each Q^2, this uncertainty affects the absolute cross section, but not the extraction of G_E/G_M.

The largest random uncertainties, where the error can differ at different ε values, are related to the tracking efficiency (0.2%), uncertainty in the scattering angle (0.2%), subtraction of the inelastic proton backgrounds (0.2%), and radiative corrections (0.2%). The total random systematic uncertainty is 0.45%, with typical statistical uncertainties of 0.25% at $Q^2 = 2.64$ GeV^2 and 0.40% at $Q^2 = 4.1$ GeV^2. Data taken at the lowest beam energy have an additional uncertainty (0.3%) because these data were taken at lower beam currents (30–50 μA), and so are sensitive to nonlinearity in the beam current measurements and have different target heating corrections.

The reduced cross sections, $\sigma_R = \tau G_M^2 + \varepsilon G_E^2$, are shown in Fig. 2. The uncertainties are the statistical and random systematic uncertainties. Some corrections lead to correction to σ_R that varies nearly linearly with ε. This modifies the slope, but does not contribute to the scatter of the points or deviations from linearity. The main uncertainties in the extracted slope come from the ε dependence of the radiative corrections (0.3%), background subtraction, (0.25%), tracking efficiency (0.25%), and the effect of beam energy or scattering angle offset (0.25%). Note that we do not include the uncertainty related to two-photon exchange, which we will discuss later. The combined 0.55% uncertainty in the slope of the reduced cross section

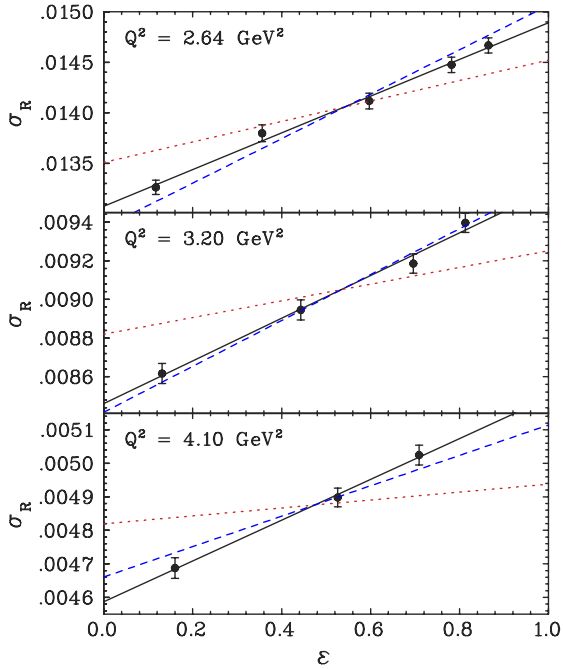

FIG. 2 (color online). Reduced cross sections as a function of ε. The solid line is a linear fit to the reduced cross sections, the dashed line shows the slope expected from scaling ($\mu_p G_E/G_M = 1$), and the dotted line shows the slope predicted by the polarization transfer experiments [6].

is included in the uncertainties of the extracted form factors.

The extracted form factors are given in Table II and shown in Fig. 3, along with the results of previous measurements. Note that for consistency with previous Rosenbluth measurements, the effects of Coulomb distortion [9] have not been included. Correcting for Coulomb distortion would lower $\mu_p G_E/G_M$ by 0.048, 0.042, and 0.032 and increase $G_M/(\mu_p G_D)$ by 0.009, 0.007, and 0.006 for $Q^2 = 2.64$, 3.2, and 4.1 GeV^2, respectively. This would reduce the ratios in Fig. 3 slightly, but still leaves a large discrepancy with the polarization transfer results.

The results presented here are in good agreement with previous Rosenbluth measurements but have much smaller statistical and systematic uncertainties. The precision of the present work leaves little room for doubting that the G_E/G_M ratios reported from polarization transfer experiments are inconsistent with those extracted from Rosenbluth separations and makes it clear that the problem is not simply experimental error in the Rosenbluth measurements. The source of this discrepancy must be identified before the new insight into the proton structure provided by the recent polarization transfer data can be fully accepted.

One possible source for the discrepancy is the effect of higher-order corrections to the Born (one-photon exchange) cross section. The form factors are extracted from the cross section (and polarization transfer) data in the Born approximation, so higher-order effects must be removed from the measured cross sections. We correct the data for bremsstrahlung, vertex corrections, and loop diagrams [8], with almost all of the ε dependence coming from bremsstrahlung. When detecting the electron, the bremsstrahlung correction yields an ε dependence to σ_R that exceeds the ε dependence coming from G_E. In this experiment, the ε-dependent correction is smaller and of the opposite sign. The consistency between the new data and previous Rosenbluth results provides a significant test of the validity of the standard bremsstrahlung corrections.

It has been suggested that higher-order processes such as two-photon exchange might explain the discrepancy [10,11]. To explain the discrepancy, such a correction would have to increase the large-ε cross sections by roughly 6% relative to the low-ε values [12], introducing large errors to the high Q^2 Rosenbluth extractions of G_E. While two-photon exchange will also affect the polarization transfer data, the corrections to the polarization transfer form factors are expected to be smaller [10,13].

Additional effort is needed to determine if the discrepancy in the form factor measurements can be explained entirely by two-photon exchange. Coulomb distortion has been examined [9] and yields only a 3%–5% reduction in G_E/G_M. Recent calculations [11,14] show significant corrections to the cross sections due to two-photon exchange, but explain only half of the observed discrepancy. Additional effort is going into calculations of two-photon exchange for the cross section and polarization transfer measurements. It remains to be seen whether two-photon exchange can resolve what must otherwise be considered a severe discrepancy.

If missing radiative correction terms are responsible for the discrepancy, then we are not correctly isolating the one-photon exchange process and the form factors extracted from a Rosenbluth separation, and to a lesser extent those taken from polarization transfer, will not correspond to the true form factors of the proton. Two-photon exchange corrections must be understood before precise comparisons can be made between models of proton structure and the measured form factors. In the meantime, it is important to be consistent in one's choice of form factors. While the form factors taken from Rosenbluth separations may not provide the true form factors, they do provide the correct e-p elastic cross section if one is working in the Born approximation with standard radiative corrections (the higher-order corrections are effectively absorbed into the form factors). Thus, the form factors from Rosenbluth extractions provide the best parametrization when elastic scattering is used to compare the normalization of different experiments, or when the elastic cross section is used as

TABLE II. Extracted form factors (and total uncertainties) relative to the dipole form, $G_D = 1/(1 + Q^2/0.71)^2$.

Q^2	2.64 GeV^2	3.20 GeV^2	4.10 GeV^2
G_E/G_D	0.949 ± 0.040	1.007 ± 0.052	1.132 ± 0.077
$G_M/(\mu_p G_D)$	1.053 ± 0.015	1.048 ± 0.015	1.031 ± 0.015
$\mu_p G_E/G_M$	0.902 ± 0.038	0.961 ± 0.051	1.097 ± 0.077

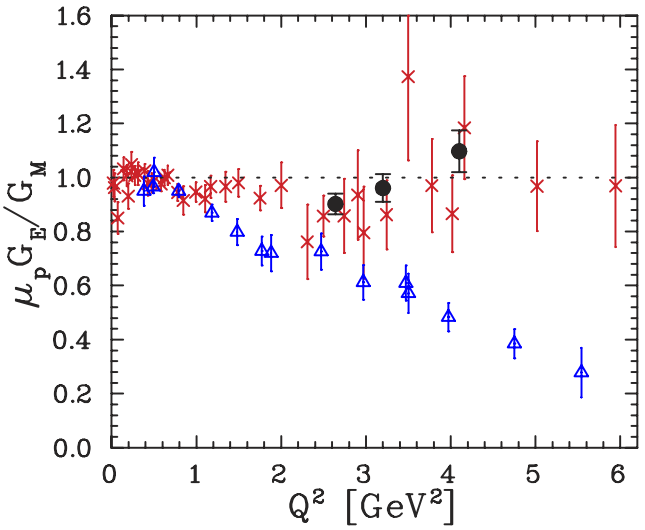

FIG. 3 (color online). Extracted values of $\mu_p G_E/G_M$ from this work (circles), a global analysis of previous cross section data (Fig. 2 of Ref. [12]) (crosses), and high-Q^2 polarization transfer measurements [5,6] (triangles).

input to the analysis of experiments such as quasielastic $A(e, e'p)$ scattering [12,15].

In conclusion, we have performed an improved Rosenbluth extraction of the proton form factors using detection of the struck proton to dramatically decrease the systematic uncertainties. The results are as precise as recent polarization transfer measurements, but are in agreement with previous Rosenbluth separations and inconsistent with high-Q^2 polarization transfer results. The precision of these new data rules out experimental error in the Rosenbluth results as the source of the discrepancy and tests the ε-dependent terms included in the standard radiative correction procedures. There are indications that this difference might come from two-photon exchange corrections, but we must better understand the discrepancy before we can be confident in our knowledge of the proton form factors.

We gratefully acknowledge the Accelerator Division, Hall A technical staff, and the members of the survey and cryotarget groups for their efforts in making this experiment possible. This work was supported in part by DOE Contract No. W-31-109-ENG-38, NSF Grants No. 0099540 and No. PHY-00-98642, NSERC (Canada), and DOE Contract No. DE-AC05-84ER40150, under which SURA operates the Thomas Jefferson National Accelerator Facility.

[1] M. N. Rosenbluth, Phys. Rev. **79**, 615 (1950).
[2] R. C. Walker *et al.*, Phys. Rev. D **49**, 5671 (1994).
[3] M. E. Christy *et al.*, Phys. Rev. C **70**, 015206 (2004).
[4] J. Arrington, Phys. Rev. C **68**, 034325 (2003).
[5] M. K. Jones *et al.*, Phys. Rev. Lett. **84**, 1398 (2000).
[6] O. Gayou *et al.*, Phys. Rev. Lett. **88**, 092301 (2002).
[7] J. Alcorn *et al.*, Nucl. Instrum. Methods Phys. Res., Sect. A **522**, 294 (2004).
[8] R. Ent *et al.*, Phys. Rev. C **64**, 054610 (2001).
[9] J. Arrington and I. Sick, Phys. Rev. C **70**, 028203 (2004).
[10] P. A. M. Guichon and M. Vanderhaeghen, Phys. Rev. Lett. **91**, 142303 (2003).
[11] P. G. Blunden, W. Melnitchouk, and J. A. Tjon, Phys. Rev. Lett. **91**, 142304 (2003).
[12] J. Arrington, Phys. Rev. C **69**, 022201(R) (2004).
[13] J. Arrington, Phys. Rev. C **71**, 015202 (2005).
[14] Y. C. Chen, A. Afanasev, S. J. Brodsky, C. E. Carlson, and M. Vanderhaeghen, Phys. Rev. Lett. **93**, 122301 (2004).
[15] D. Dutta *et al.*, Phys. Rev. C **68**, 064603 (2003).